jove

Assembly and Operation of an Acoustofluidic Device for Enhanced Delivery of Molecular Compounds to Cells

Connor S. Centner[1], **Emily M. Murphy**[1], **Bryce F. Stamp**[2], **Mariah C. Priddy**[1], **John T. Moore**[1], **Paula J. Bates**[2], **Michael A. Menze**[3], **Kavitha Yaddanapudi**[2], **Jonathan A. Kopechek**[1]

[1] Department of Bioengineering, University of Louisville [2] School of Medicine, University of Louisville [3] Department of Biology, University of Louisville

Corresponding Author

Jonathan A. Kopechek
jonathan.kopechek@louisville.edu

Citation

Centner, C.S., Murphy, E.M., Stamp, B.F., Priddy, M.C., Moore, J.T., Bates, P.J., Menze, M.A., Yaddanapudi, K., Kopechek, J.A. Assembly and Operation of an Acoustofluidic Device for Enhanced Delivery of Molecular Compounds to Cells. *J. Vis. Exp.* (167), e62035, doi:10.3791/62035 (2021).

Date Published

January 21, 2021

DOI

10.3791/62035

URL

jove.com/video/62035

Abstract

Efficient intracellular delivery of biomolecules is required for a broad range of biomedical research and cell-based therapeutic applications. Ultrasound-mediated sonoporation is an emerging technique for rapid intracellular delivery of biomolecules. Sonoporation occurs when cavitation of gas-filled microbubbles forms transient pores in nearby cell membranes, which enables rapid uptake of biomolecules from the surrounding fluid. Current techniques for in vitro sonoporation of cells in suspension are limited by slow throughput, variability in the ultrasound exposure conditions for each cell, and high cost. To address these limitations, a low-cost acoustofluidic device has been developed which integrates an ultrasound transducer in a PDMS-based fluidic device to induce consistent sonoporation of cells as they flow through the channels in combination with ultrasound contrast agents. The device is fabricated using standard photolithography techniques to produce the PDMS-based fluidic chip. An ultrasound piezo disk transducer is attached to the device and driven by a microcontroller. The assembly can be integrated inside a 3D-printed case for added protection. Cells and microbubbles are pushed through the device using a syringe pump or a peristaltic pump connected to PVC tubing. Enhanced delivery of biomolecules to human T cells and lung cancer cells is demonstrated with this acoustofluidic system. Compared to bulk treatment approaches, this acoustofluidic system increases throughput and reduces variability, which can improve cell processing methods for biomedical research applications and manufacturing of cell-based therapeutics.

Introduction

Viral and non-viral platforms have been utilized to enhance molecular delivery to cells. Viral delivery (transduction) is a common technique utilized in cell-based therapies requiring genomic modification. Limitations with viral delivery include

potential insertional mutagenesis, limited transgenic capacity, and undesired multiplicity of infection[1,2]. Therefore, non-viral molecular delivery techniques are in development for a broad range of biomedical and research applications. Common techniques include mechanical, electrical, hydrodynamic, or the use of laser-based energy to enhance uptake of biomolecules into cells [3]. Electroporation is a commonly used non-viral molecular delivery platform which has the ability to induce transient perforation in the plasma membrane for intracellular delivery of molecular compounds[4,5,6,7,8,9]. However, the transient perforation of the plasma membrane is a stochastic process and molecular uptake via electroporation is generally dependent on passive diffusion across the transient membrane pores[4,7,8].

An alternative method is the utilization of ultrasound for enhanced intracellular molecular delivery via cavitation of ultrasound contrast agents (i.e., gas-filled microbubbles). Microbubble cavitation induces microstreaming effects in the surrounding media which can cause transient perforation of nearby plasma membranes ("sonoporation") allowing rapid intracellular uptake of biomolecules via passive or active transport mechanisms[10,11,12]. Sonoporation is an effective technique for the rapid molecular delivery to cells, but this approach often requires expensive equipment and bulk treatment methods which are limited by lower throughput and higher variability in ultrasound exposure conditions[13]. To address these limitations, acoustofluidic devices, which enable consistent sonoporation of cells in suspension, are currently in development.

Acoustofluidics is an expanding field that integrates ultrasound and microfluidic technologies for a wide variety of applications. This approach has previously been used for particle separation by applying continuous ultrasound energy to induce standing acoustic waves within the fluidic channels[14,15,16,17]. Particles are sorted toward different parts of the device based on a variety of properties such as particle size, density, and compressibility relative to the medium[16]. Acoustofluidic technologies are also in development to enable rapid molecular delivery to a variety of cell types for research applications and manufacturing of cell therapies[18]. Recently, we demonstrated enhanced molecular delivery to erythrocytes using a PDMS-based acoustofluidic device[19]. In the acoustofluidic platform, cell and microbubble dynamics can be manipulated to induce physical interactions that enable enhanced delivery of biomolecules. The efficiency and consistency of intracellular molecular delivery can potentially be increased by optimizing the distance between cells and microbubbles.

One important application for acoustofluidic-mediated sonoporation involves transport of biomolecules into primary human T cells. Immunotherapies based on adoptive T cell transfer, such as Chimeric Antigen Receptor T cell (CAR T) therapy, are rapidly emerging for treatment of various diseases, including cancer and viruses such as HIV[20]. CAR T therapy has been particularly effective in pediatric acute lymphoblastic leukemia (ALL) patients, with complete remission rates of 70-90%[21]. However, T cell manufacturing for these therapies generally depends on viral transduction which is limited by potential insertional mutagenesis, long processing times, and challenges of delivering non-genetic biomolecules such as proteins or small molecules[1]. Acoustofluidic-mediated molecular delivery methods can potentially overcome these limitations and improve manufacturing of T cell therapies.

Another important application for acoustofluidic-mediated sonoporation involves intracellular delivery of preservative

compounds, such as trehalose, which protect cells during freezing and desiccation. Trehalose is produced by some organisms in nature and helps them tolerate freezing and desiccation by protecting their cellular membranes[22,23]. However, trehalose is not produced by mammalian cells and is impermeable to mammalian cell membranes. Therefore, effective molecular delivery techniques, such as sonoporation, are necessary in order to achieve sufficient intracellular trehalose levels required to protect internal cellular membranes. This approach is currently in development for dry preservation of various cell types.

This protocol provides a detailed description of the assembly and operation of a relatively low-cost acoustofluidic system driven by a microcontroller. Ultrasound contrast agents are utilized to induce sonoporation within the fluidic channels and enable rapid molecular delivery to various cell types, including T cells and cancer cells. This acoustofluidic system can be used for a variety of research applications and may also be useful as a prototype system to evaluate sonoporation methods for improved cell therapy manufacturing processes.

Protocol

Whole blood donations were collected from healthy donors following protocols approved by the institutional review board at the University of Louisville.

1. Fabrication of acoustofluidic device

1. Obtain a photomask with a concentric spiral design containing channels with a diameter of 500 µm. A CAD file is provided in the supplemental files as an example. A custom photomask can be ordered from a commercial vendor or patterned using a mask writer.
2. Prepare a mold of the concentric spiral design on a photoresist-coated silicon wafer using standard photolithography techniques.
    1. Add approximately 2 Tbsp (~30 mL) of SU-8 2100 to a 100 mm silicon wafer.
    2. Spin-coat the wafer on a spinner at a speed of 150 rpm for 30 s to spread out the photoresist, then increase the speed to 1,200 rpm for 60 s to yield a thickness of 200 µm.
    3. Cure the photoresist-coated wafer in a polyimide vacuum oven with a 30 min ramp up and 30 min dwell at 115 °C, then ramp down for 30 min.
    4. Expose the photoresist-coated wafer for 130 s using a mask aligner with the photomask from step 1.1.
    5. Bake the wafer after exposure following the same process described in step 1.2.3.
    6. Develop the photoresist in SU-8 developer solution for approximately 8 min.
    CAUTION: Only use developer solution in a well-ventilated chemical fume hood.
3. Silanize the mold to make the surface more hydrophobic. Place the photoresist-coated wafer into a desiccator and add a 20 µL drop of chlorosilane ($C_8H_4Cl_3F_{13}Si$). Apply vacuum to the chamber for 30 s, then seal the chamber and leave overnight.
CAUTION: Chlorosilane is very hazardous and flammable. Exposure causes severe burns and eye damage.
4. Combine 54 g of polydimethsiloxane (PDMS) base and 6 g of curing agent in a cup and mix vigorously and thoroughly with a spatula for at least 1 min.

5. Place the cup containing the PDMS solution into a desiccator for approximately 30 min or until remnant air bubbles are removed from the solution.
6. Place photoresist-coated wafer with the patterns facing upward in a 150-mm Petri dish.
7. Pour the PDMS solution over the mold inside the 150-mm Petri dish.
8. If needed, place the 150-mm Petri dish inside a desiccator and apply vacuum until remnant air bubbles disappear.
9. Transfer the 150-mm Petri dish into a lab oven and bake for 2 h at 60 °C to cure the PDMS.
10. After curing, carefully remove the PDMS from the Petri dish by cutting around the edges of the wafer using a razor blade.
11. Cut out each individual device using a knife or razor blade.
12. Punch holes through the inlet and outlet ports of each device using a 2.5-mm biopsy punch.
13. Place each PDMS device in a plasma asher with channels exposed (facing upward). Apply oxygen plasma treatment (100 W for 45 s, 500 mbar O_2) then immediately place each PDMS device onto a clean soda lime glass microscope slide (75 mm x 25 mm x 1 mm) with channels facing the glass surface.
14. Let devices bond overnight at room temperature.
15. Gently apply silicone to the surface of the 1-cm diameter piezo transducer at a thickness of ~1-2mm, then carefully align the transducer with the concentric spiral and gently press it onto the bottom of the glass microscope slide (opposite side from the PDMS device).

2. Assembly and operation of acoustofluidic system

1. Connect a microcontroller to a computer using a USB A to B cable. A green power LED indicator (labeled PWR) should illuminate.
2. Use the associated program on the computer to upload a program which generates an 8 MHz signal. An example program is provided in the **Supplemental Files**. After uploading the program, it will be stored into microprocessor memory and will not need to be uploaded again.
3. Solder a 1" 22G wire to the end of each wire on the PZT transducer.
4. Connect the negative (black) terminal wire of PZT transducer to a GND pin via the soldered wire.
5. Connect the positive (red) terminal wire of PZT transducer to the output pin (#9 in the provided example program) via the soldered wire.
6. Optionally, mount the acoustofluidic device and the microcontroller in a 3D-printed case. CAD files are provided in the **Supplemental Files** as examples. Additional wires can be connected to other microcontroller pins to control an external LED indicator and on/off push button if desired.
7. Cut 3-6" sections of tygon PVC soft plastic tubing (1/16" ID, 1/8" OD) and push the tubing into the inlet and outlet ports. It may be necessary to rotate the tubing while applying pressure until it fits in the opening. Optionally, after inserting the tubing into each port, glue can be applied at the junction to bond the PDMS and tubing together.
8. Assemble the microfluidic reservoir according to manufacturer's instructions.

9. Cut a 3-6" section of tygon PVC soft plastic tubing (1/16" ID, 1/8" OD) and push the tubing over the 1/32" ID tubing from the microfluidic reservoir output tubing. Optionally, wrap the junction with paraffin film to prevent leakage.
10. Fill a 60-mL syringe with ambient air (optionally, filter the air with a 0.2-µm filter) and connect it to tygon PVC tubing (1/16" ID, 1/8" OD) on the side of the microfluidic reservoir.
11. Set the syringe pump to a rate of 200 mL/h to push the cell/ultrasound contrast agent solutions through the acoustofluidic device at a volumetric flow rate of 50 mL/h and collect the samples from the output of the acoustofluidic device into a 50mL centrifuge tube. Optionally, rinse channel prior to acoustofluidic treatment with 15 mL of 70% ethanol solution to increase sterility of fluidic channels. Additionally, channels can be rinsed with 15 mL of deionized water to remove residual ethanol in the device prior to pumping cells through the system.

3. Preparation of ultrasound contrast agents

NOTE: Ultrasound contrast agents significantly enhance acoustofluidic delivery of molecular compounds by transiently increasing permeabilization of nearby cellular membranes[19]. Molecular delivery is very limited without ultrasound contrast agents in this system.

1. Prepare a phospholipid solution in a 20mL scintillation vial containing the following mixture:
    1. Add 25 mg of 1,2-distearoyl-sn-glycero-3-phosphocholine (DSPC).
    2. Add 11.6 mg of 1,2-distearoyl-sn-glycero-3-ethylphosphocholine (DSEPC).
    3. Add 0.26 mg of 1,2-distearoyl-sn-glycero-3-phosphoglycerol (DSPG).
    4. Add 0.88 mg of polyoxyethylene40 stearate.
2. Add chloroform until all phospholipids are dissolved (e.g., 3 mL of chloroform).
3. Evaporate chloroform in a desiccator for 48 h to form a dry lipid film (evaporation under argon or with a rotary evaporator can be used to accelerate the drying process).
4. Rehydrate the lipid film with 10 mL of sterile phosphate-buffered saline (PBS).
5. Sonicate the lipid solution for 3 min at 40% amplitude to form a cationic micellar solution.
6. After sonication store the phospholipid solution at 2-6 °C for up to 1 month.
7. To prepare ultrasound contrast agents, add 200 µL of cationic micellar solution and 600 µL of sterile PBS to a 2 mL glass septum vial.
8. Seal the vial by crimping the cap.
9. Use a 1.5" 20G needle to fill the vial head space with decafluorobutane gas for 30 s.
10. Amalgamate the vial for 45 s at 4,350 cpm to form perfluorobutane gas-filled ultrasound contrast agents.
11. Add 25 µL of ultrasound contrast agent solution per 1 mL of cell solution immediately before pumping the combined contrast agent/cell mixture through the acoustofluidic device. The cell solution can be modified as desired by the user, but in our studies the cell solution consisted of primary T cells in step 4.21, and A549 lung cancer cells in step 5.7, respectively.

4. Preparation of primary Tcells

1. Isolate peripheral blood mononuclear cells (PBMCs) from whole blood solutions and store at -150 °C. Density gradient separation containing a substrate is commonly utilized to separate PBMCs from whole blood[24,25,26].
2. Thaw frozen vial in 37 °C water bath.
3. Dilute thawed PBMCs 1:10 with PBS in a 15mL centrifuge tube. Each 1mL vial contains approximately 10 million PBMCs.
4. Centrifuge diluted PBMCs at 580 x *g* for 11 min at 4 °C.
5. Aspirate the supernatant and add 13 mL of MACs running buffer to resuspend the cells.
6. Count the PBMCs with an automated cell counter or hemocytometer.
7. Centrifuge the PBMCs again at 580 x *g* for 11 min at 4 °C and aspirate the supernatant.
8. Add 40 µL of chilled running buffer per 10 million PBMCs.
9. To isolate T cells, add 10 µL of Pan T-Cell Biotin Antibody Cocktail per 10 million PBMCs.
10. Gently agitate the PBMCs and store the solution at 4 °C for 5 min per 10 million cells.
11. Add 30 µL of running buffer and 20 µL of Pan T-Cell MicroBead Cocktail per 10 million PBMCs.
12. Mix the PBMCs and beads thoroughly and incubate for an additional 15 min at 4 °C.
13. Add running buffer to reach a total volume of 500 µL.
14. Separate primary T cells with a commercially available benchtop magnetic sorting instrument using the "depletes separation" setting following manufacturer's protocol. This step should yield between 5-10 million T cells after cell sorting.
15. Count T cells using an automated cell counter or hemocytometer.
16. Dilute T cells in 10 mL of sterile PBS and centrifuge at 580 x g for 10 min at 4 °C to pellet the cells.
17. Aspirate the supernatant and resuspend T cells in 1 mL of PBS.
18. Count T cells using an automated cell counter or hemocytometer and aliquot 1 million/mL for experiments.
19. Prepare a 1 mg/mL fluorescein solution in PBS.
20. Add 100 µL of 1 mg/mL fluorescein solution per 1 mL of T cell solution (final fluorescein concentration = 100 µg/mL) immediately prior to processing.
21. Add 25 µL of ultrasound contrast agent solution as previously described in step 3.11.
22. Process 1mL aliquots of cells using the acoustofluidic system (see steps 2.10-2.11). This step enhances delivery of fluorescein into primary T cells.
23. Immediately after treatment, wash cells three times via centrifugation at 580 x *g* for 10 min with 500 µL of PBS to remove extracellular fluorescein. Cells should be washed within 10 min after adding fluorescein solution.
24. After final washing step, resuspend cells in 250 µL of PBS and measure fluorescence on flow cytometer.

5. Preparation of A549 lung cancer cells

1. Culture A549 (adenocarcinomic human alveolar basal epithelial) cells in complete DMEM media (10% fetal bovine serum, 1% penicillin/streptomycin) at 37 °C and 5% CO_2 in a flat-bottom tissue culture flask.

2. Harvest A549 cells when they reach 70-90% confluency. Aspirate media from the flask and wash the cells once with PBS to remove serum proteins.
3. Add trypsin (0.25%) EDTA to the flask and incubate for 5 min at 37 °C. Trypsin is a digestive enzyme which causes the cells to detach from the bottom surface of the tissue culture flask.
4. Transfer trypsin solution to a 15mL centrifuge tube and neutralize it by adding complete DMEM media at a 1:3 ratio.
5. Pellet the cells via centrifugation at 1,500 x *g* for 5 min at 4 °C.
6. Aspirate the supernatant and resuspend the pellet at a concentration of 100,000/mL in PBS solution containing 200 mM trehalose in 15-mL conical vial.
7. Add 25 µL of ultrasound contrast agent solution as previously described in step 3.11.
8. Process 1mL aliquots of cells using the acoustofluidic system (see steps 2.10-2.11). This step enhances delivery of trehalose into A549 lung cancer cells.
9. Immediately after treatment, wash cells three times via centrifugation with 500 µL of PBS to remove extracellular trehalose. Cells should be washed within 10 min after adding trehalose solution.
10. After final washing step, resuspend cells in 100 µL of PBS.
11. Add 11 µL of 1% Triton X-100 solution to lyse cells and release intracellular trehalose.
12. Vortex for 15 s, then incubate for 30 min at room temperature.
13. Vortex again for 15 s, then measure trehalose concentration using commercially available trehalose assay following manufacturer's recommendation.

Representative Results

An image of the acoustofluidic system assembled inside a 3D-printed case is shown in **Figure 1**. This protocol produces an acoustofluidic system that can be used to enhance intracellular molecular delivery in multiple cell lines using ultrasound contrast agents.

Figure 2 demonstrates enhanced intracellular delivery of a fluorescent compound, fluorescein, to primary human T cells with acoustofluidic treatment compared to an untreated control group ($p<0.05$, n=3/group). T cells were suspended at a concentration of 1 million/mL in PBS with 100 µg/mL fluorescein solution and 25 µL/mL ultrasound contrast agent solution, and the mixture was passed through the acoustofluidic device for ultrasound treatment. Intracellular fluorescein delivery and cell viability were measured with flow cytometry after washing cells via centrifugation to remove extracellular fluorescein. T cells in the untreated control group were also suspended at 1 million/mL in PBS with 100 µg/mL fluorescein solution, but ultrasound contrast agent solution was not added and cells were not passed through the acoustofluidic device. The fluorescence intensity of T cells increased by 5-fold after acoustofluidic treatment relative to the fluorescence intensity of T cells in the untreated control group, indicating enhanced delivery of fluorescein. Cell viability decreased slightly after acoustofluidic treatment but remained above 80% ($p<0.05$, n=3/group).

Figure 3 demonstrates enhanced intracellular delivery of a preservative compound, trehalose, to human A549 lung carcinoma cells with acoustofluidic treatment compared to

flow alone (no ultrasound contrast agents or ultrasound exposure) and compared to cells in the untreated control group (ANOVA $p<0.05$, n=3/group). A549 cells were suspended at a concentration of 100,000/mL in PBS with 200 mM trehalose solution and 25 µL/mL ultrasound contrast agent solution, and the mixture was passed through the acoustofluidic device for ultrasound treatment. A549 cells in the control groups ("Flow Only" and "No Treatment") were also suspended at 100,000/mL in PBS with 200 mM trehalose, but ultrasound contrast agent solution was not added and cells were not exposed to ultrasound treatment. Intracellular trehalose was quantified using a trehalose assay kit and normalized to the untreated control group. Cell viability was measured with trypan blue assay. There was no statistical difference in cell viability between groups (n=3-7/group).

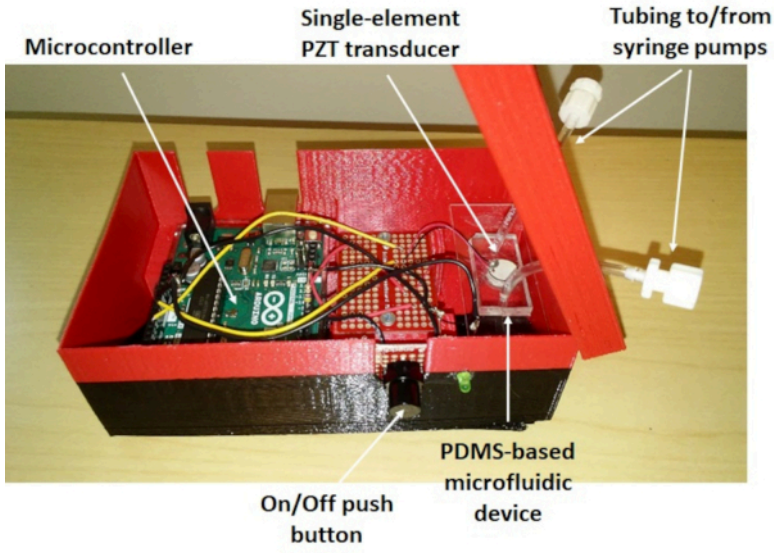

Figure 1: Photo of acoustofluidic system. The acoustofluidic flow system contains a PDMS-based flow chamber with an integrated PZT transducer driven by a microcontroller. A 3D-printed case with an LED indicator and on/off push button are optional additional features. Please click here to view a larger version of this figure.

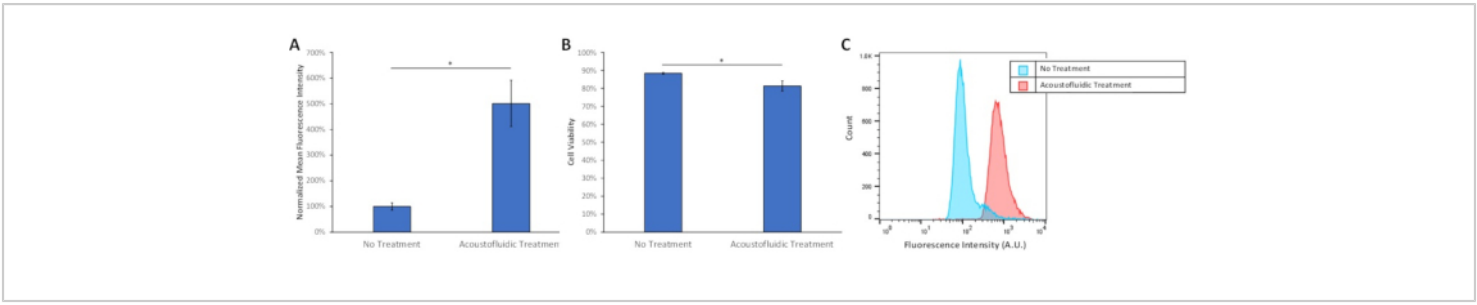

Figure 2: Acoustofluidic treatment enhances fluorescein delivery to human T cells. (**A**) Fluorescence intensity in primary T cells increased after acoustofluidic treatment with fluorescein compared to the untreated control group (no acoustofluidics and no microbubbles) (p<0.05, n=3/group). (**B**) Cell viability decreased slightly after acoustofluidic treatment but remained above 80% as measured by flow cytometry (p<0.05, n=3/group). (**C**) Representative flow cytometry histogram indicating higher fluorescence in the acoustofluidic treatment group. Please click here to view a larger version of this figure.

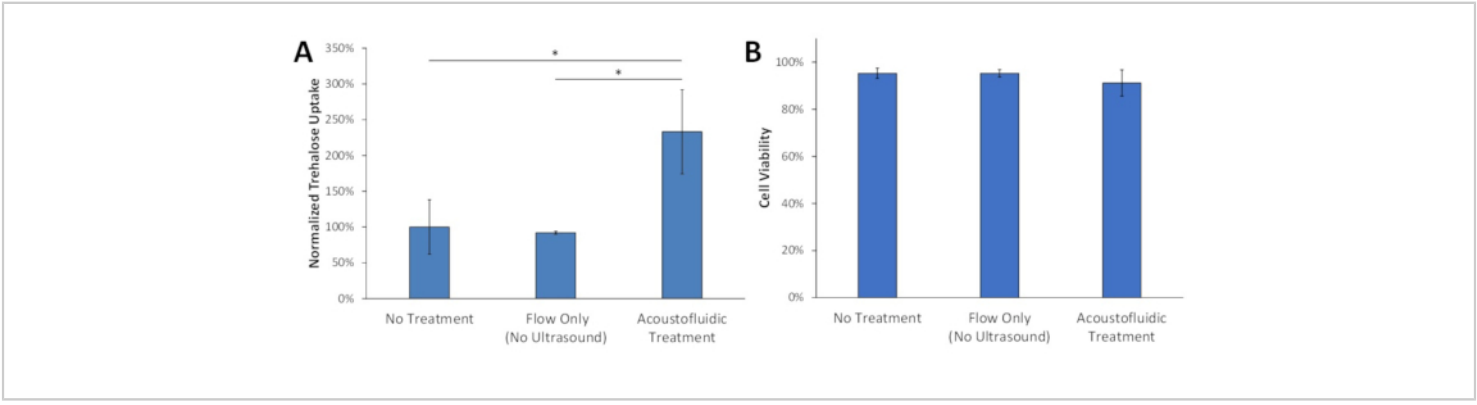

Figure 3: Acoustofluidic treatment enhances trehalose delivery to human lung cancer cells. (**A**) Trehalose uptake increased in A549 lung carcinoma cells compared to flow only (no ultrasound and no microbubbles) and the untreated control group (ANOVA p<0.05, n=3/group). (**B**) Cell viability remained above 90% after acoustofluidic treatment as measured by trypan blue assay (n=3-7/group). Please click here to view a larger version of this figure.

Supplemental files. Please click here to download this file.

Discussion

This protocol describes the assembly and operation of a low-cost acoustofluidic system which enhances intracellular delivery of biomolecules for research applications. There are several important factors to consider when assembling and operating this system. The acoustofluidic device is fabricated in PDMS, which is a biocompatible material that can easily be molded with consistent channel dimensions[27].The device channels can be rinsed with 15 mL of 70% ethanol solution prior to acoustofluidic processing in order to increase sterility when working with cultured cells. Following ethanol cleaning, 15 mL of deionized water can be used to rinse the device to remove residual ethanol from the channels prior to adding cell solutions. Small acoustofluidic channels can easily

become blocked by debris or cell aggregates, making this a limitation for the frequent use of the device. Thoroughly rinsing the channels between each sample will help prevent problems with channel blockage. In addition, multiple PDMS devices can be fabricated in each batch so that devices can be quickly replaced if necessary. For ultrasound-based applications, it is important to produce PDMS devices with a consistent thickness, as differences in PDMS thickness can affect the ultrasound pressures within the fluidic channels. Ultrasound waves propagate continuously through the device and transmitted waves interact with reflected waves to form standing acoustic wave patterns that are very sensitive to differences in PDMS thickness[17].The PDMS thickness is primarily determined by the amount of PDMS added to the mold (step 1.7) and this protocol yields a PDMS thickness of 3.5 mm.

The maximum output frequency of the microcontroller (8 MHz) was selected to produce the smallest acoustic wavelength within the fluidic channel. The microcontroller output is typically a square wave but oscilloscope measurements revealed that the output at 8 MHz becomes more similar to a sinusoid waveform due to slew rate limitations. A limitation of this system is that the maximum voltage output of the microcontroller is 5V and an external RF amplifier is required if higher voltage outputs are desired. The free-field pressure output of the transducer in this system was 18 kPa at 1 cm as measured with a needle hydrophone (Precision Acoustics, Dorchester, United Kingdom). Although this pressure is relatively low, standing waves within the channels can increase the acoustic pressures which samples are exposed to as they pass through the ultrasound beam.

Ultrasound contrast agents are used to nucleate acoustic cavitation within the acoustofluidic channels which enhances delivery of biomolecules across cell membranes[28,29]. This protocol describes synthesis of perfluorocarbon gas-filled microbubbles encapsulated by a cationic phospholipid membrane. As previously described, this formulation consists of microbubbles primarily between 1-3 µm in diameter[30]. The positively charged surface of the microbubbles attracts them toward negatively-charged cell membranes, which increases sonoporation-mediated molecular delivery when the microbubbles and cells are in close proximity. The concentration of microbubbles in the cell solution is a critical factor that can influence the efficiency of molecular delivery and cell viability after acoustofluidic treatment, and the optimal microbubble concentration may be specific to each cell type [19]. The concentration of gas-filled microbubbles with a lipid shell can decrease over time after synthesis so ultrasound contrast agents should be used within a few hours after synthesis.

We demonstrated delivery of a fluorescent compound (fluorescein) to primary non-activated human T cells using the acoustofluidic system in this protocol. It is important to note that the activation status of primary human T cells may affect the efficiency of intracellular molecular delivery. The fluorescence properties of fluorescein enable sensitive intracellular detection with flow cytometry, but other soluble compounds can also be delivered into cells using this acoustofluidic system. For example, we demonstrated acoustofluidic delivery of trehalose into human lung cancer cells. Acoustofluidic delivery of trehalose into cells may enable increased recovery after frozen and dry storage, which could have significant impacts on a range of biomedical and research applications [19].

Acoustofluidic delivery of other biomolecules, such as proteins or DNA plasmids, is also possible, although

a limitation of this system is that the efficiency of molecular delivery may be lower for larger compounds[18,31]. Optimization of acoustofluidic flow rate, concentrations of ultrasound contrast agents, cell concentrations, and media may be needed for delivery of other biomolecules. In addition, optimal parameters may vary between different cell types due to factors such as cell diameter, morphology, membrane properties, and phenotype.

The acoustofluidic system described in this protocol can be easily assembled and operated at relatively low cost. Additionally, this system can be customized for other applications by connecting other signal sources or ultrasound transducers to generate specific output pressures and frequencies[32,33,34]. In addition, the syringe pump system described in this protocol can be replaced with peristaltic pumps if desired. At a flow rate of 50 mL/h the residence time for cells within the ultrasound beam as they pass through the acoustofluidic channel is approximately 1 s, but this residence time can be modified as needed for specific applications by adjusting the fluid flow rate.

Unlike other common transfection techniques, biomolecules can be delivered into cells within minutes instead of hours and this system does not require specialized and expensive equipment. In addition, this system is compatible with a wide range of commonly used cell culture media or other buffers. In summary, this acoustofluidic system enables rapid delivery of biomolecules to cells, which may be useful for a wide range of research applications.

Disclosures

Co-authors MAM and JAK hold ownership in DesiCorp which may financially benefit from products related to this research.

Acknowledgments

This work was supported in part by funding from the National Science Foundation (#1827521, #1827521, #1450370) and the National Institutes of Health (U01HL127518). Photolithography services were provided by the University of Louisville Micro/Nano Technology Center.

References

1. Gardlik, R. et al. Vectors and delivery systems in gene therapy. *Medical Science Monitor.* **11** (4), RA110-RA121 (2005).
2. Wahlers, A. et al. Influence of multiplicity of infection and protein stability on retroviral vector-mediated gene expression in hematopoietic cells. *Gene Therapy.* **8** (6), 477-486 (2001).
3. Nayerossadat, N., Maedeh, T., Ali, P. A. Viral and nonviral delivery systems for gene delivery. *Advanced Biomedical Research.* **1**, 27 (2012).
4. Chen, C., Smye, S. W., Robinson, M. P., Evans, J. A. Membrane electroporation theories: a review. *Medical & Biological Engineering & Computing.* **44** (1-2), 5-14 (2006).
5. Gehl, J. Electroporation: theory and methods, perspectives for drug delivery, gene therapy and research. *Acta Physiologica Scandinavica.* **177** (4), 437-447 (2003).
6. Lin, Y. C., Li, M., Wu, C. C. Simulation and experimental demonstration of the electric field assisted electroporation microchip for in vitro gene delivery enhancement. *Lab on a Chip.* **4** (2), 104-108 (2004).

7. Sugar, I. P., Neumann, E. Stochastic model for electric field-induced membrane pores. Electroporation. *Biophysical Chemistry.* **19** (3), 211-225 (1984).
8. Weaver, J. C. Electroporation: a general phenomenon for manipulating cells and tissues. *Journal of Cellular Biochemistry.* **51** (4), 426-435 (1993).
9. Hashimoto, M., Takemoto, T. Electroporation enables the efficient mRNA delivery into the mouse zygotes and facilitates CRISPR/Cas9-based genome editing. *Scientific Reports.* **5**, 11315 (2015).
10. Klibanov, A. L. Microbubble contrast agents: targeted ultrasound imaging and ultrasound-assisted drug-delivery applications. *Investigative Radiology.* **41** (3), 354-362 (2006).
11. Klibanov, A. L., Shevchenko, T. I., Raju, B. I., Seip, R., Chin, C. T. Ultrasound-triggered release of materials entrapped in microbubble-liposome constructs: a tool for targeted drug delivery. *Journal of Controlled Release.* **148** (1), 13-17 (2010).
12. Fan, Z., Kumon, R. E., Deng, C. X. Mechanisms of microbubble-facilitated sonoporation for drug and gene delivery. *Therapeutic Delivery.* **5** (4), 467-486 (2014).
13. Secomski, W. et al. In vitro ultrasound experiments: Standing wave and multiple reflections influence on the outcome. *Ultrasonics.* **77**, 203-213 (2017).
14. Gedge, M., Hill, M. Acoustofluidics 17: theory and applications of surface acoustic wave devices for particle manipulation. *Lab on a Chip.* **12** (17), 2998-3007 (2012).
15. Shi, J. et al. Acoustic tweezers: patterning cells and microparticles using standing surface acoustic waves (SSAW). *Lab on a Chip.* **9** (20), 2890-2895 (2009).
16. Shi, J., Huang, H., Stratton, Z., Huang, Y., Huang, T. J. Continuous particle separation in a microfluidic channel via standing surface acoustic waves (SSAW). *Lab on a Chip.* **9** (23), 3354-3359 (2009).
17. Shields, C. W. t., Cruz, D. F., Ohiri, K. A., Yellen, B. B., Lopez, G. P. Fabrication and operation of acoustofluidic devices supporting bulk acoustic standing waves for sheathless focusing of particles. *Journal of Visualized Experiments.* (109), e53861 (2016).
18. Belling, J. N. et al. Acoustofluidic sonoporation for gene delivery to human hematopoietic stem and progenitor cells. *Proceedings of the National Academy of Sciences.* **117** (20), 10976-10982 (2020).
19. Centner, C. S. et al. Ultrasound-induced molecular delivery to erythrocytes using a microfluidic system. *Biomicrofluidics.* **14** (2), 024114 (2020).
20. Qi, J., Ding, C., Jiang, X., Gao, Y. Advances in developing CAR T-cell therapy for HIV cure. *Frontiers in Immunology.* **11**, 361 (2020).
21. Annesley, C. E., Summers, C., Ceppi, F., Gardner, R. A. The evolution and future of CAR T cells for B-Cell Acute lymphoblastic leukemia. *Clinical Pharmacology & Therapeutics.* **103** (4), 591-598 (2018).
22. Hand, S. C., Menze, M. A. Molecular approaches for improving desiccation tolerance: insights from the brine shrimp Artemia franciscana. *Planta.* **242** (2), 379-388 (2015).
23. Zhang, M. et al. Freeze-drying of mammalian cells using trehalose: preservation of DNA integrity. *Scientific Reports.* **7** (1), 6198 (2017).
24. Grievink, H. W., Luisman, T., Kluft, C., Moerland, M., Malone, K. E. Comparison of three isolation techniques

for human peripheral blood mononuclear cells: Cell recovery and viability, population composition, and cell functionality. *Biopreserv Biobank.* **14** (5), 410-415 (2016).

25. Jaatinen, T., Laine, J. Isolation of mononuclear cells from human cord blood by Ficoll-Paque density gradient. *Current Protocol in Stem Cell Biology.* **Chapter 2,** Unit 2A 1, (2007).
26. Ulmer, A. J., Scholz, W., Ernst, M., Brandt, E., Flad, H. D. Isolation and subfractionation of human peripheral blood mononuclear cells (PBMC) by density gradient centrifugation on Percoll. *Immunobiology.* **166** (3), 238-250 (1984).
27. Halldorsson, S., Lucumi, E., Gomez-Sjoberg, R., Fleming, R. M. T. Advantages and challenges of microfluidic cell culture in polydimethylsiloxane devices. *Biosensors and Bioelectronics.* **63**, 218-231 (2015).
28. Helfield, B., Chen, X., Watkins, S. C., Villanueva, F. S. Biophysical insight into mechanisms of sonoporation. *Proceedings of the National Academy of Sciences.* **113** (36), 9983-9988 (2016).
29. Hu, Y., Wan, J. M., Yu, A. C. Membrane perforation and recovery dynamics in microbubble-mediated sonoporation. *Ultrasound in Medicine and Biology.* **39** (12), 2393-2405 (2013).
30. Kopechek, J. A. et al. Ultrasound targeted microbubble destruction-mediated delivery of a transcription factor decoy inhibits STAT3 signaling and tumor growth. *Theranostics.* **5** (12), 1378-1387 (2015).
31. Bhutto, D. F. et al. Effect of molecular weight on sonoporation-mediated uptake in human cells. *Ultrasound in Medical Biology.* **44** (12), 2662-2672 (2018).
32. Forbes, M. M., Steinberg, R. L., O'Brien, W. D., Jr. Frequency-dependent evaluation of the role of definity in producing sonoporation of Chinese hamster ovary cells. *Journal of Ultrasound in Medicine.* **30** (1), 61-69 (2011).
33. Helfield, B., Chen, X., Watkins, S. C., Villanueva, F. S. Biophysical insight into mechanisms of sonoporation. *Proceedings of National Academy of Science U. S. A.* **113** (36), 9983-9988 (2016).
34. Miller, D. L., Bao, S., Morris, J. E. Sonoporation of cultured cells in the rotating tube exposure system. *Ultrasound in Medical Biology.* **25** (1), 143-149 (1999).